Journal of Applied Physics

Interplay of vacancies, hydrogen, and electrical compensation in irradiated and annealed *n*-type β-Ga_2O_3

Cite as: J. Appl. Phys. **129**, 165702 (2021); https://doi.org/10.1063/5.0042518
Submitted: 31 December 2020 . Accepted: 31 March 2021 . Published Online: 23 April 2021

A. Karjalainen, P. M. Weiser, I. Makkonen, V. M. Reinertsen, L. Vines, and F. Tuomisto

ARTICLES YOU MAY BE INTERESTED IN

Zn acceptors in β-Ga_2O_3 crystals
Journal of Applied Physics **129**, 155701 (2021); https://doi.org/10.1063/5.0047947

Analysis of tunable Bleustein–Gulyaev permittivity sensors
Journal of Applied Physics **129**, 164501 (2021); https://doi.org/10.1063/5.0041505

Superlens coupling to object and image: A secondary resonance mechanism to improve single-negative imaging of electromagnetic waves
Journal of Applied Physics **129**, 163102 (2021); https://doi.org/10.1063/5.0040060

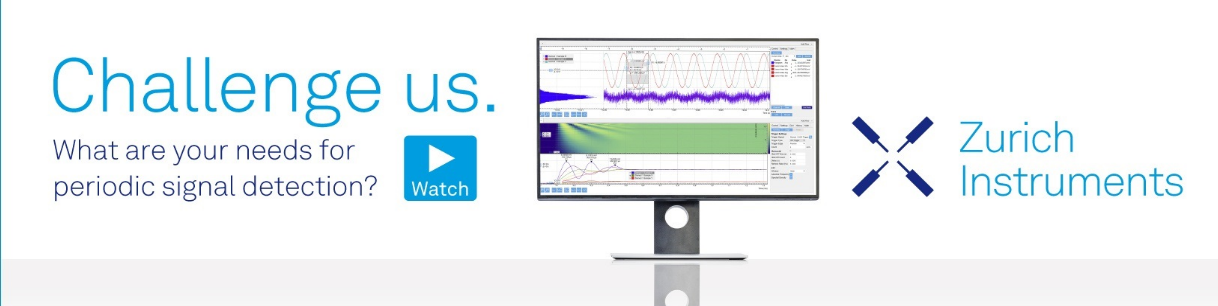

© 2021 Author(s).

Journal of Applied Physics ARTICLE scitation.org/journal/jap

Interplay of vacancies, hydrogen, and electrical compensation in irradiated and annealed *n*-type β-Ga_2O_3

Cite as: J. Appl. Phys. **129**, 165702 (2021); doi: 10.1063/5.0042518
Submitted: 31 December 2020 · Accepted: 31 March 2021 ·
Published Online: 23 April 2021

A. Karjalainen,[1,2,a)] P. M. Weiser,[3] I. Makkonen,[2,4] V. M. Reinertsen,[3] L. Vines,[3] and F. Tuomisto[1,2,4]

AFFILIATIONS

[1]Department of Applied Physics, Aalto University, P.O. Box 15100, FI-00076 Aalto, Espoo, Finland
[2]Department of Physics, University of Helsinki, P.O. Box 43, FI-00014 Helsinki, Finland
[3]Department of Physics, Centre for Materials Science and Nanotechnology, University of Oslo, Blindern P.O. Box 1048, Oslo, Norway
[4]Helsinki Institute of Physics, P.O. Box 64, FI-00014 Helsinki, Finland

[a)]**Author to whom correspondence should be addressed:** antti.j.karjalainen@iki.fi

ABSTRACT

Positron annihilation spectroscopy, Fourier transform-infrared absorption spectroscopy, and secondary ion mass spectrometry have been used to study the behavior of gallium vacancy-related defects and hydrogen in deuterium (D) implanted and subsequently annealed β-Ga_2O_3 single crystals. The data suggest the implantation generates a plethora of V_{Ga}-related species, including V_{Ga1}- and V_{Ga2}-type defects. The latter's contribution to the positron signal was enhanced after an anneal at 300 °C, which is driven by the passivation of V_{Ga}^{ib} by hydrogen as seen from infrared measurements. Subsequent annealing near 600 °C returns the positron signal to levels similar to those in the as-received samples, which suggests that split V_{Ga}-like defects are still present in the sample. The almost complete removal of the V_{Ga}^{ib}-2D vibrational line, the appearance of new weak O-D lines in the same spectral region, and the lack of D out-diffusion from the samples suggest that the 600 °C anneal promotes the formation of either D-containing, IR-inactive complexes or defect complexes between V_{Ga}^{ib}-2D and other implantation-induced defects. The degree of electrical compensation is found to be governed by the interactions between the Ga vacancies and hydrogen.

Published under an exclusive license by AIP Publishing. https://doi.org/10.1063/5.0042518

I. INTRODUCTION

β-Ga_2O_3 is an ultrawide bandgap (4.9 eV) semiconductor with a high theoretical electric breakdown field (8 MV cm^{-1}), which gives it excellent potential as a successor for GaN and SiC in UV and high power electronics applications.[1] *N*-type doping can be achieved with Sn or Si doping[1,2] with typical carrier concentrations[1] in the range of 10^{16}–10^{19} cm^{-3}, which has led to the development of a number of unipolar devices.[3] However, an understanding of the mechanisms that lead to *compensation* of the *n*-type conductivity is not very well established. In particular, electrical measurements[4] show that proton irradiation strongly decreases the charge carrier concentration, presumably by the formation of compensating acceptors. A compensating acceptor with an optical threshold at ≈2 eV below the conduction band minimum was reported by several authors.[5–8] Recent investigations using steady-state photocapacitance measurements[9] tentatively assigned this signature to a Ga-related primary intrinsic defect. Indeed, theory[4,10] finds that gallium vacancies (V_{Ga}) are deep acceptors and therefore likely candidates for these species. These observations are consistent with the results of early positron annihilation spectroscopy (PAS) experiments,[11] where a strong correlation between V_{Ga} and the degree of compensation of *n*-type conductivity[12,13] was seen. Recent studies utilizing deep-level transient spectroscopy (DLTS) have shown that irradiation also gives rise to two charge state transition levels labeled E2* and E4.[4,14–16] Annealing the samples at 600 K removes the E4 level but also increases the concentration of E2*.[4] In fact, E2* has been shown to limit the performance β-Ga_2O_3-based metal-semiconductor field

Published under an exclusive license by AIP Publishing.

effect (MESFET) transistors[17,18] and suggested to originate from V_{Ga}-V_{O} divacancy defect complexes.[16,19]

One of the difficulties in studying intrinsic point defects in β-Ga_2O_3 is the large number of V_{Ga} configurations. Theory finds that monovacancies of both of the inequivalent Ga sites (V_{Ga1} and V_{Ga2}), are metastable, and exhibit rather low energy barriers (<0.5 eV) to relax into "split vacancy" (or shifted) configurations (V^{i}_{Ga}) in n-type materials.[4,10] Scanning transmission electron microscopy[20] has observed both these V^{i}_{Ga} defects and their complexes with Sn dopants in as-grown single crystals. Furthermore, a higher Sn concentration appears to enhance the V^{i}_{Ga} concentration, which was also suggested by theory.[4,10] Electron paramagnetic resonance (EPR) studies[21–23] have found two defect signals labeled as EPR1 and EPR2 from which EPR1 was recently suggested to arise from V^{ib}_{Ga} or V_{Ga1}. Recent positron annihilation studies show that V^{i}_{Ga} can be present in high concentrations ($\gtrsim 1 \times 10^{18}\,cm^{-3}$) in as-received β-Ga_2O_3 single crystals regardless of the growth method or doping concentration.[24,25] Fourier transform-infrared (FT-IR) spectroscopy is often used to study hydrogen (H)-related defects via the absorption of localized O-H vibrations. Although H and D generally exhibit similar physical behaviors, D is often used as a probe in place of H due to its higher sensitivity in certain techniques, e.g., FT-IR and secondary ion mass spectrometry (SIMS). A number of OH-related defects have been reported in β-Ga_2O_3 [26–29] and the dominant defect has been identified from the polarization properties of the vibrational line to be V^{ib}_{Ga}-2H.[26,27] The diffusion of D in ion-implanted β-Ga_2O_3 single crystals was investigated using SIMS[30,31] and shown to be highly anisotropic and limited by intrinsic defects that serve as traps for D.[32] The traps could be present in as-received crystals, consistent with the recent positron annihilation results.

In this work, we combined positron annihilation spectroscopy, FT-IR spectroscopy, and SIMS to study the evolution of V_{Ga} and H/D in β-Ga_2O_3 single crystals after D implantation and subsequent thermal annealing. We utilize state-of-the-art theoretical calculations of positron annihilation signals for detailed analysis of the experimental data. First, it is found that irradiation creates a multitude of V_{Ga}-related defects, including those containing V_{Ga1}- and V_{Ga2}-type defects. Annealing at 300 °C was found to increase the irradiation-generated defect positron signal and also to strongly enhance the intensity of the V^{ib}_{Ga}-2D vibrational line. Interestingly, the electrical conductivity lost in the irradiation is actually recovered in the annealing at 300 °C. Annealing at near 600 °C returns the positron signal to that seen in the as-received sample. The anneal also results in the complete disappearance of the V^{ib}_{Ga}-2D line and the appearance of new O-D-related vibrational lines, suggesting that H is released from V^{ib}_{Ga} and forms IR-inactive species while V^{ib}_{Ga} are still present in the samples. The combination of data from each technique implies that both hydrogen and (split) Ga vacancies, together with their mutual passivation, have a strong influence on the electrical conductivity in n-type β-Ga_2O_3.

II. METHODS

The β-Ga_2O_3 bulk single crystals studied in this work were grown by the edge-defined film-fed growth method (Tamura Corporation). All samples were single side polished and had the $(\bar{2}01)$ surface orientation. N-type samples doped with Sn (carrier concentration of $8 \times 10^{18}\,cm^{-3}$) were used for PAS and SIMS measurements. However, the strong free-carrier absorption in these samples prevented IR transmittance measurements of the spectral region where O-D stretching vibrations occur. Therefore, unintentionally doped (UID) samples (carrier concentration of $1 \times 10^{18}\,cm^{-3}$) with either the $(\bar{2}01)$ or (010) surface orientation were used for FT-IR measurements. The different surface orientations were used to ensure that all possible O-D dipole moments could be detected.

To study irradiation-generated vacancies, Sn-doped samples were implanted from the polished surface at room temperature with 1.1 MeV D^+ ions with a fluence of $2 \times 10^{15}\,cm^{-2}$. The UID samples used for FT-IR measurements were implanted with the same fluence but at a lower energy (200 keV). The D implantation peak in the 1.1 MeV D^+-implanted samples is located approximately 8 μm below the sample surface, leading to a fairly homogeneous damage profile up to 4 μm. To investigate the effects of annealing, the irradiated samples were annealed in air inside a tube furnace at temperatures between 300 and 625 °C for 30 min.

Doppler broadening of positron-electron annihilation radiation was measured similarly to Ref. 25 with a variable energy slow positron beam. We note here that the resolution of the high-purity Ge detector was 1.25 keV at 511 keV, the detector was mounted perpendicular to the beamline and the detector–sample distance is ~3 cm. The S and W parameter integration windows were set as 0–0.45 and 1.5–4.1 a.u., respectively. A second W parameter was defined as 2.0–4.1 a.u. and referred to as $W2$ throughout this work, similarly to Ref. 25. We show data obtained at a positron implantation energy of 25 keV, where the effect of surface annihilations was insignificant and the stopping depths are less than 3 μm, staying within the homogeneous defect profile generated by the D implantation. 5×10^6 counts were accumulated in the 511 keV annihilation peak in each spectrum and the statistical error estimates of the acquired S, W, and $W2$ parameters are approximately 2×10^{-4}, 1×10^{-4}, and 5×10^{-5}, respectively.

To check how the formation of complexes with Sn may affect the positron signals of Ga vacancy defects, we performed first-principles calculations fully consistent with earlier work, described in detail in Ref. 24. We considered the experimentally observed $2V_{Ga1}$-Sn_{ib} and $2V_{Ga1}$-Sn_{ic} complexes in the −2 charge state, and their hydrogenated counterparts ($2V_{Ga1}$-Sn_{ib}-2H and $2V_{Ga1}$-Sn_{ic}-2H, respectively) at zero charge state, in monoclinic 160-atom supercells.[4,20,24] Figure 1 shows the crystallographic orientations along which the experimental and theoretically calculated (S, W, $W2$) parameters are determined.

FT-IR measurements were performed at 5.0 K at a spectral resolution of 0.5 cm^{-1} and with the IR beam at normal incidence on the polished sample surface. The samples were cooled in He exchange gas in a Janis PTSHI-950-5 low vibration, pulse tube cryostat equipped with ZnSe windows. The IR spectra were acquired using a Bruker IFS 125HR spectrometer equipped with a globar source, a KBr beam splitter, and a liquid nitrogen-cooled InSb detector. The spectra were corrected to remove the sloping baseline arising from absorption due to free carriers and from scattering at the rough back surface. A calibration of the effective charge, q, for the 2546-cm^{-1}-V^{ib}_{Ga}-2D line (at 5 K) is presented in Sec. III C,

Published under an exclusive license by AIP Publishing.

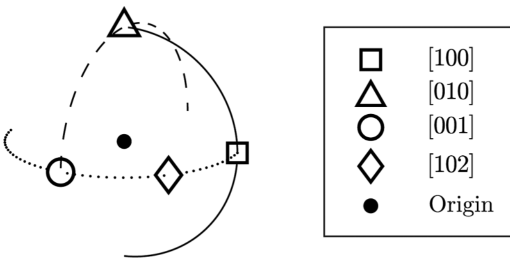

FIG. 1. The notation of the measurement directions for the (S, W, $W2$) parameters. The markers represent the given lattice directions and the full, dashed, and dotted lines scans along the three "geodesics" which connect [100], [010], and [001] lattice directions.[24]

using the equation[33]

$$q^2 = \frac{2.303mnc^2}{\pi Nd}\int A(\bar{v})d\bar{v}, \quad (1)$$

where m is the mass of the oscillating impurity (D), n is the refractive index at the wavenumber where the impurity oscillates, c is the speed of light, N is the concentration of V_{Ga}^{ib}-2D, and d is the thickness of the implanted region.

Concentration vs depth profiles of D were measured using SIMS after post-implantation heat treatments at temperatures between 300 and 625 °C. The detection limit of D in the SIMS measurements was $<5 \times 10^{15}$ cm^{-3}, with a vacuum of $<1 \times 10^{-9}$ mTorr in the sample chamber. Further details about the SIMS setup and the measurements can be found in Ref. 32. In general, the electrical conductivity at the surface of the as-implanted samples was too low to permit SIMS measurements. Post-implantation annealing restored the conductivity to a level such that SIMS measurements were possible on the Sn-doped samples, but generally not on the UID samples. However, one SIMS measurement was obtained for a D-implanted ($\bar{2}01$) UID sample after subsequent 30-min anneals at 300 and 400 °C. The integrated D concentration-depth profile from this measurement gives the quantity Nd used in Eq. (1).

III. RESULTS

A. Positron annihilation spectroscopy

Figure 2 shows the (S, W) and (S, $W2$) parameters measured in the as-received, irradiated, and annealed β-Ga_2O_3 samples in the [010] and [102] lattice directions. Clearly, the irradiation increases S and decreases the W and $W2$ parameters irrespective of measurement direction, indicative of introduced vacancy-type defects. Annealing at 300 °C effectively doubles the original effect of the irradiation on the (S, W, $W2$) parameters. After annealing at 625 °C, the (S, W, $W2$) parameters are very close to those of the as-received samples, suggesting recovery of the irradiation-induced vacancy defects.

Interestingly, the (S, W, $W2$) parameters evolve clearly more in the [102] than in the [010] direction after irradiation and annealing, equivalent to a significant change in the degree of anisotropy in

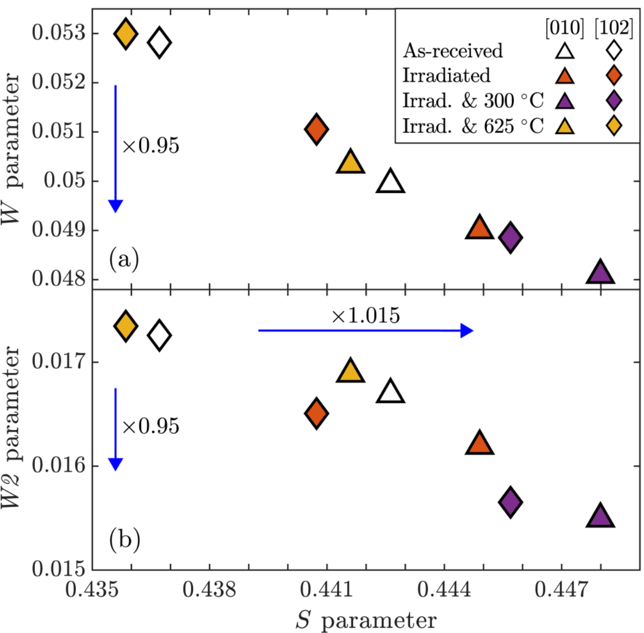

FIG. 2. (a) (S, W) parameters and (b) (S, $W2$) parameters measured in the as-received, irradiated, and annealed samples in the [010] (triangles) and [102] lattice directions (diamonds). Blue scale bars are drawn to guide the eye. The error estimates are smaller than the markers and are not drawn.

the signals. In the as-received and 625 °C annealed samples, the overall anisotropy in the S parameter is roughly 1.015, defined as the highest (lowest) value divided by the lowest (highest) value of the S (W, $W2$) parameter, as discussed in Ref. 24. In the W and $W2$ parameters, the anisotropy is 0.95 and 0.96, respectively. After irradiation, the anisotropy in S and W is reduced by roughly 30%, followed by a reduction of a similar magnitude after the 300 °C anneal. The anisotropy in the $W2$ parameter is reduced much more, essentially vanishing after the 300 °C anneal. Analysis of the Doppler broadening lineshapes and the (S, W, $W2$) parameters suggests the data of the irradiated sample is a roughly 50/50 superposition of the data of the as-received and 300 °C annealed samples, meaning that the vacancy signal introduced in the irradiated sample is enhanced after the 300 °C anneal.

The evolution of the experimental (S, W, $W2$) parameters can be compared to the theoretically predicted parameters of various types of defects. Figure 3 shows the calculated (S, W) and (S, $W2$) parameters projected in the [010] and [102] lattice directions for V_{Ga}^{ib} with 0-2 hydrogen atoms and both unrelaxed V_{Ga} defects, according to Ref. 24. The differences in the typical behavior of the anisotropy visible in the (S, W, $W2$) between the split Ga vacancies and unrelaxed Ga vacancies are notably similar to the experimentally observed difference between as-received (and 625 °C annealed) and the irradiated and 300 °C samples. This suggests that unrelaxed Ga vacancies are introduced in the irradiation. Note that the positron signals of the as-received samples are dominated by the split Ga vacancies, as shown in Ref. 25.

Published under an exclusive license by AIP Publishing.

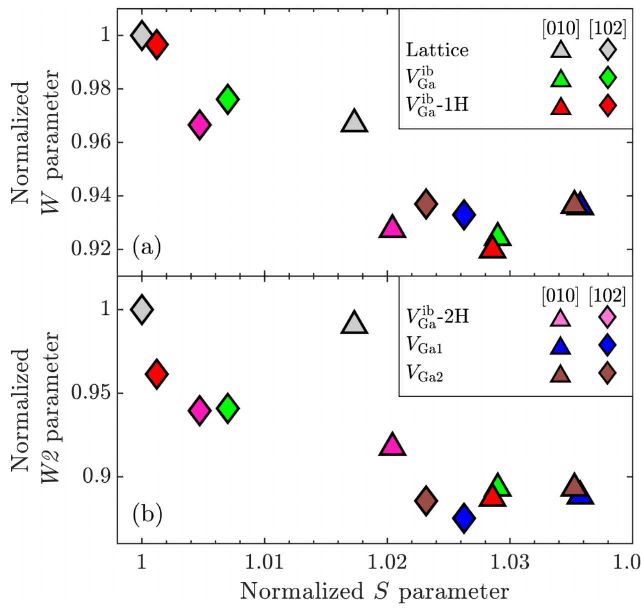

FIG. 3. (a) (*S*, *W*) parameters and (b) (*S*, *W2*) parameters calculated for the V_{Ga}^{ib} and V_{Ga} defects in the [010] (triangles) and [102] lattice directions (diamonds). The data in the [102] lattice direction are averaged in the plane spanned by the [100] and [001] lattice directions to take into account the aspect ratio of the positron beam and the effect of the unit cell, described in detail in Ref. 24.

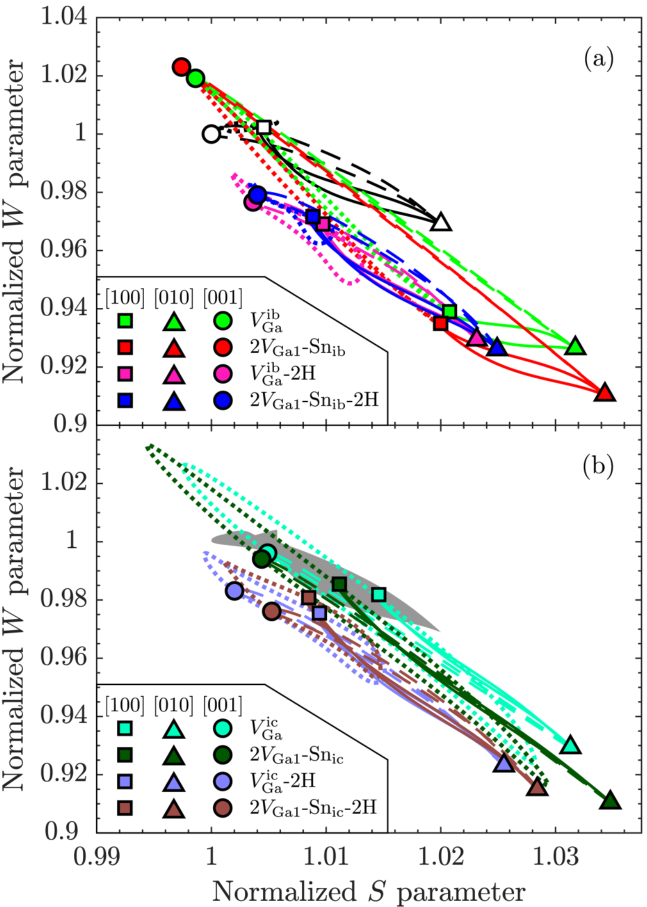

FIG. 4. Calculated (*S*, *W*) parameters of V_{Ga}^{ib}, V_{Ga}^{ib}-2H, V_{Ga}^{ic}, and V_{Ga}^{ic}-2H with and without Sn. The β-Ga_2O_3 lattice signal is shown for comparison[24] in (a) with white symbols and in (b) as a gray shadow. The full, dashed, and dotted lines follow the notation introduced in Fig. 1. Complexing with Sn has a negligible effect on the (*S*, *W*) parameters of split Ga vacancies.

To check the possible effect of Sn replacing Ga as the center interstitial atom in the split Ga vacancies[20] on the positron annihilation signals, we calculated the full anisotropy in the *ib* and *ic* split Sn-Ga vacancies with and without hydrogen. The results are shown in Fig. 4 and compared to their Sn-free counterparts calculated in Ref. 24. It is clear that the effect of Sn on the (*S*, *W*) parameters is minimal, slightly increasing the overall anisotropy, but not changing its nature in any way. Hence, the evolution of the experimental positron annihilation signals in irradiation and annealing should not be related to interactions between Sn and Ga vacancies. Note that the effect of Sn on the calculated positron lifetimes (not shown) is also minimal, resulting in at most 2 ps increase compared to the values in Ref. 24.

B. FT-IR spectroscopy

Figure 5 shows IR absorbance spectra for a $(\bar{2}01)$-oriented β-Ga_2O_3 sample in the spectral region where O-D stretching vibrations occur after D implantation and subsequent heat treatments. No O-D or O-H-related vibrational lines were detected in the as-received samples. The as-implanted sample exhibits several absorption lines that are positioned at 2518, 2546, 2567, 2578, 2591, and 2632 cm^{-1}. The dominant line at 2546 cm^{-1} originates from V_{Ga}^{ib}-2D.[26,27] The 300 °C annealing increases the intensity of the 2546 cm^{-1} line at the expense of the intensities of the other O-D lines. Subsequent anneals at higher temperatures up to 700 °C cause the intensity of the 2546 cm^{-1} line to decrease considerably and also result in the appearance of absorption lines at 2476, 2532, 2542, and 2639 cm^{-1}. The assignment of these new absorption lines to O-D stretching modes was recently reported by Portoff *et al.*[29] Importantly, the spectra in Fig. 5 show how the dominant O-D species in the implanted region is controlled by the post-implantation annealing temperature. Similar results are obtained for the (010)-oriented sample, i.e., none of the vibrational lines have a dipole moment oriented along [010].

The integrated absorbance of the 2546-cm^{-1} V_{Ga}^{ib}-2D line for probing light along the [102] axis after the 300 °C anneal is 0.023 cm^{-1}. The dipole moment of this defect is at an angle of 15° from the [102] axis, which results in a correction to the integrated absorbance, to 0.025 cm^{-1}. The D concentration-depth profile (not shown) for this sample yields $N_D d = 4.07 \times 10^{15}$ cm^{-2}. This value should be divided by two because the defect in question contains two D atoms. Assuming an isotropic medium for the refractive

Published under an exclusive license by AIP Publishing.

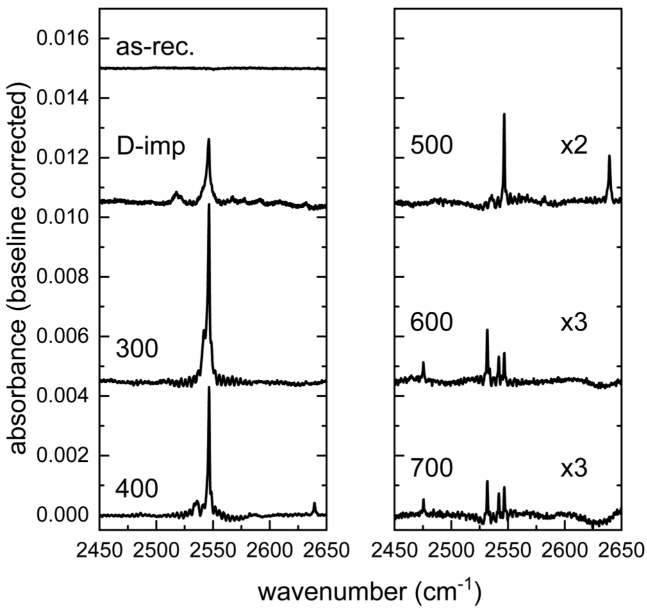

FIG. 5. Baseline-corrected IR absorbance spectra at 5 K of a ($\bar{2}01$)-oriented β-Ga_2O_3 sample in the as-received state and after implantation and subsequent isochronal anneals (30 min) at temperatures between 300 and 700 °C.

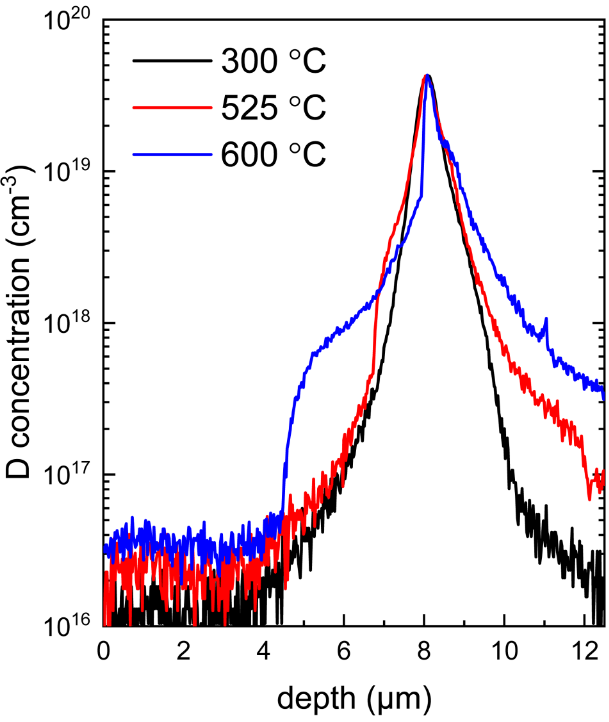

FIG. 6. D concentration-depth profiles for a ($\bar{2}01$)-oriented β-Ga_2O_3 single crystal after D implantation and subsequent isochronal anneals (30 min) at 300, 525, and 600 °C.

index ($n = 1.88$) and that all of the D is trapped at V_{Ga}^{ib} after the 300 °C anneal, the effective charge (for probing light along [102]) is determined to be (0.47 ± 0.05) e. The corresponding concentration of V_{Ga}^{ib}-2D (in the implantation peak) after the 300 °C anneal is 1.3×10^{19} cm^{-3}, which is in excellent agreement with the value estimated from the implantation conditions (fluence of 2×10^{15} cm^{-2} and an implanted region with thickness of 1.5 μm). The detection limit is estimated to be $\sim 1 \times 10^{17}$ cm^{-3} in a 1.5 μm thick layer (the detection limit scales inversely proportional to the layer thickness).

C. Secondary ion mass spectrometry

Figure 6 shows D concentration vs depth profiles in D-implanted, Sn-doped β-Ga_2O_3 samples after post-implantation heat treatments at 300, 525, and 600 °C. The 300 °C anneal shows a well-defined implantation peak located approximately 8 μm below the surface with a maximum D concentration of 4×10^{19} cm^{-3}. Diffusion of D into the bulk β-Ga_2O_3 is observed after the 525 °C anneal, whereas noticeable diffusion toward the surface is also seen after the 600 °C anneal. Reinertsen *et al.*[32] showed recently that the D concentration-depth profiles can be modeled by trap-limited diffusion, where the diffusion of D is controlled by its capture and release from traps present either in the as-received samples or after ion implantation. The height of the diffusion front on either side of the implantation peak can be used to estimate the concentration of trap(s) present in the sample. A trap concentration (between the surface and the implantation peak) in the order of 10^{18} cm^{-3} is estimated from the 600 °C profile shown in Fig. 6. Notably, the SIMS profiles imply that the positron measurements do not probe the region with implanted D even after the highest-temperature annealing.

IV. DISCUSSION

The positron results show that as-received samples show the strongest Doppler broadening signal anisotropy and, upon irradiation, a larger change in (*S*, *W*) parameters in [102] than in the [010] lattice direction, which are both in agreement with the theoretical[24] and experimental[25] positron work where a high concentration of split Ga vacancies of type V_{Ga}^{ib} or V_{Ga}^{ic} were identified in as-received β-Ga_2O_3 single crystals. The D implantation introduces vacancy defects with a higher *S* parameter (lower *W* and *W2*) and a significantly smaller Doppler signal anisotropy than those in the as-received sample, in agreement with the annihilation parameters predicted for V_{Ga1} and V_{Ga2}. However, first-principles calculations[10,34] predict that unrelaxed V_{Ga}, i.e., V_{Ga1} and V_{Ga2}, are metastable configurations, and should already be able to overcome the relatively low barriers (<0.5 eV) to relax into the split configurations at room temperature. Furthermore, the calculated O-D stretch modes of D-containing unshifted V_{Ga1} and V_{Ga2} defects should be polarized along the [010] lattice vector,[26,27,35] but the O-D vibrational lines observed in implanted samples (ours and Ref. 29) are not polarized along [010]. Recent first-principles calculations by Fowler *et al.* showed that H trapping and relaxation processes in β-Ga_2O_3 make it highly unlikely

Published under an exclusive license by AIP Publishing.

that any of the hydrogenated unshifted V_{Ga} will occur.[35] Interestingly, recent experimental[16] and theoretical work[19] have suggested that V_{Ga}-V_O divacancy complexes could give rise to the so-called E2* level observed using DLTS in β-Ga_2O_3 single crystals after H- and He-irradiation. Importantly, the positron annihilation signature of a cation vacancy is expected to remain relatively unchanged compared to its complex with a small anion vacancy.[25,36] Therefore, the changes to the positron signals after irradiation could originate from creation of V_{Ga}-V_O complexes containing V_{Ga1} and V_{Ga2}.

Samples annealed at 300 °C can be probed by SIMS, PAS, and FT-IR. The SIMS profile (black curve) shown in Fig. 6 shows a well-defined D implantation peak centered approximately 8 μm below the sample surface, which is consistent with SRIM simulations.[37] For positrons, the 300 °C annealing further increases S parameter (decreases W and $W2$) and reduces the Doppler signal anisotropy. A thorough analysis of the Doppler spectral shape suggests that this change is due increased positron trapping at the irradiation-generated V_{Ga1}- and V_{Ga2}-like defects, rather than a change in their structure or creation of new V_{Ga} defects. The observed anisotropy in the 300 °C-annealed sample is also comparable to the anisotropy predicted for V_{Ga1}- and V_{Ga2}-like defects, which suggests that the positron trapping to these vacancies could be near saturation ($>1 \times 10^{18}$ cm^{-3}). One plausible explanation for the increased trapping at the irradiation-induced V_{Ga1}- and V_{Ga2}-like defects is that other positron traps, e.g., split V_{Ga}, become less efficient due to H passivation. Indeed, theoretical work[11,38] suggests that twofold H/D passivation reduces the positron trapping coefficient of cation vacancies (V_{Ga}^{ib}-2H) by a factor of ~10 due to the reduced remaining open volume and the more positive charge. Therefore, the higher fraction of positrons that are trapped at V_{Ga1}- or V_{Ga2}-like defects enhances their contribution to the positron signal. Ingebritsen *et al.*[4] proposed passivation of V_{Ga} acceptors by H as a potential explanation for the charge carrier recovery observed in H^+-implanted and annealed β-Ga_2O_3 single crystals. Indeed, passivation of split V_{Ga} by hydrogen (H/D) is qualitatively consistent with the FT-IR data in Fig. 5, which shows an increase in the intensity of the 2546.4-cm^{-1} V_{Ga}^{ib}-2D line by almost a factor of 3. This increase is accompanied by the disappearance of other O-D vibrational lines seen after implantation. Evidently, the charge carrier recovery does not require the removal of unrelaxed V_{Ga} defects, but rather the passivation of V_{Ga}^{i}-type defects, and suggests that H plays a significant role in determining the degree of compensation, as proposed in Refs. 12, 13, and 24.

The above-mentioned interpretation of the positron data after the 300 °C anneal requires a concentration of H or D in the order of ~10^{18} cm^{-3} in the region probed by positrons. The SIMS data in Fig. 6 show that the concentration of D in the damage track is nearly two orders of magnitude lower than this, which implies that the ~10^{18} cm^{-3} is determined by H present in the as-grown material. Hydrogen and silicon were proposed to be the two main impurities responsible for the unintentional n-type conductivity in β-Ga_2O_3.[2,39–44] Indeed, Czochralski-grown β-Ga_2O_3 single crystals were shown to contain substantial contributions to the free electron concentration arising from H incorporated during growth and at concentrations (10^{17}–10^{18} cm^{-3}) that are consistent with the PAS results.[40] As stated above, the strong free-carrier absorption prevents investigation of the 3437 cm^{-1} V_{Ga}^{ib}-2H line in the Sn-doped samples, but it is completely absent in the UID samples even after post-implantation annealings. If one assumes that the residual H concentration is similar in both Sn-doped and UID samples, then the FT-IR data suggest a residual H concentration well below that needed to explain the PAS results. However, we cannot exclude the possibility that there is a difference in the residual H concentration between the UID and Sn-doped samples, or that H is present as an IR-inactive species, e.g., H_2. Further investigations are needed to clarify this discrepancy.

The positron data after the 625 °C anneal are similar to the data for the as-received samples. The disappearance of the irradiation-generated V_{Ga} signals implies that these defects are either partially or entirely removed by the anneal, which could occur either by diffusing out of the probing region or by relaxing to the energetically-favorable split V_{Ga} configurations.[4,10] We analyze the thermal annealing kinetics similarly as Kyrtsos *et al.*[34] by assuming a typical phonon frequency of 1×10^{13} Hz as an approximation for the attempt frequency and 1 Hz as the estimate reaction rate where recovery is visible. We observe the recovery of regular vacancies at a temperature between 300 and 625 °C. These temperatures correspond to 1.5 and 2.3 eV, respectively, hence the migration barrier for the irradiation-generated vacancy defects can be estimated as (1.9 ± 0.4) eV. The 2546 cm^{-1} line disappears from the spectrum, and weak O-D lines appear in its vicinity, which have been speculated to arise from complexes between V_{Ga}^{ib}-2D and other defects created by implantation.[29] The SIMS results in Fig. 6 show that the majority of the implanted D is still present in the sample, and, therefore, the out-diffusion of D cannot explain the disappearance of the 2546 cm^{-1} line. The positron results indicate that defects with signatures matching those of split V_{Ga} are still present after the 625 °C annealing, which is in agreement with the suggestion by Ref. 29. Therefore, the combination of positron annihilation, SIMS, and FT-IR data suggest that D (or whole V_{Ga}^{ib}-2D defects) are present in a different, IR-inactive configuration after the 625 °C anneal. These configurations are either not able to trap positrons efficiently, and therefore do not affect the positron signal, or have positron signals that closely resemble those of split V_{Ga}.

Last, we note that the observed evolution of split and unrelaxed Ga vacancies and their interactions with hydrogen provide strong evidence for these point defects determining the degree of compensation in n-type β-Ga_2O_3. Importantly, as observed already earlier, the originally n-type conductive β-Ga_2O_3 samples become highly resistive or even semi-insulating after the irradiation, which renders electrical measurements (e.g., DLTS) impossible[4] and causes charging problems in SIMS. Annealing at 300 °C restores the conductivity, but as seen in our present results, the irradiation-induced Ga vacancies have not recovered. This means that the compensation caused by the introduction of unrelaxed Ga vacancies is canceled out by the motion of hydrogen into vacancy defects. Further investigations are required to identify the detailed mechanisms behind the compensation, but it is clear that the interplay of (split) Ga vacancies and hydrogen plays a decisive role.

V. SUMMARY

In summary, positron annihilation, FT-IR, and SIMS have been combined to study the evolution of V_{Ga} and hydrogen in β-Ga_2O_3 single crystals after D-implantation and subsequent

Published under an exclusive license by AIP Publishing.

thermal annealing. The positron annihilation data suggest that the D-implantation creates defects that contain unrelaxed V_{Ga}, and experimental and theoretical results in the literature point toward V_{Ga}-V_O divacancies as the possible candidates for these species. The presence of several types of V_{Ga}-related defects is also confirmed by FT-IR from the presence of multiple O-D-related vibrational lines present in the as-implanted sample. The 300 °C anneal enhances the intensity of the 2546-cm^{-1} V_{Ga}^{ib}-2D vibrational line by a factor of 3, which suggests that the other O-D-related defects provide a source of D that can passivate V_{Ga}^{ib} created during implantation or present in the as-received sample. The passivation of V_{Ga}^{ib} by hydrogen (H/D) suppresses its ability to capture positrons, thereby allowing their capture by V_{Ga1}- and V_{Ga2}-related defects. Although these techniques are in qualitative agreement for this explanation, additional investigations are needed to clarify the apparent quantitative discrepancy. The anneal at 625 °C returns the positron signals back to the levels in the as-received samples and also results in relatively small but visible diffusion of D. The lack of D out-diffusion, the still remaining strong split Ga vacancy-associated positron signal, the almost complete removal of the 2546-cm^{-1} line, and the appearance of several new O-D-related vibrational lines is consistent with the release of D from V_{Ga}^{ib} to form different, IR-inactive species; the formation of larger defect complexes between V_{Ga}^{ib}-D and other implantation-induced point defects; or a combination of the two. This study provides new insights and considerations for future studies of V_{Ga}-type defects and their interaction with hydrogen. In particular, their interplay in determining the degree of compensation of n-type β-Ga_2O_3 appears key to understanding the electrical characteristics of this material.

ACKNOWLEDGMENTS

We wish to thank Y. K. Frodason for sharing unpublished results about V_{Ga}-V_O defects. We are also grateful to M. Stavola and W. B. Fowler for sharing their manuscript on H/D implantations in β-Ga_2O_3 prior to publication, as well as for helpful discussions regarding the calibration of the V_{Ga}^{ib}-2D vibrational line. The authors gratefully acknowledge the computational resources provided by the CSC (Finnish IT Centre for Science). This work was partially supported by the Academy of Finland Grant Nos. 285809, 315082, and 319178. A. K. wishes to thank the Magnus Ehrnrooth foundation for financial support. The work at the University of Oslo was supported by the Research Council of Norway by the Norwegian Micro- and Nano-Fabrication Facility (NorFab No. 295864), the Functionalizing Defects in Advanced Semiconductors (FUNDAMENT No. 251131), and the Research Center for Sustainable Solar Cell Technology (FME SUSOLTECH No. 257639).

DATA AVAILABILITY

The data that support the findings of this study are available from the corresponding author upon reasonable request.

REFERENCES

[1] S. Pearton, J. Yang, P. H. Cary, IV, F. Ren, J. Kim, M. J. Tadjer, and M. A. Mastro, "A review of Ga_2O_3 materials, processing, and devices," Appl. Phys. Rev. **5**, 011301 (2018).

[2] J. Zhang, J. Shi, D.-C. Qi, L. Chen, and K. H. L. Zhang, "Recent progress on the electronic structure, defect, and doping properties of Ga_2O_3," APL Mater. **8**, 020906 (2020).

[3] M. Higashiwaki, H. Murakami, Y. Kumagai, and A. Kuramata, "Current status of Ga_2O_3 power devices," Jpn. J. Appl. Phys. **55**, 1202A1 (2016).

[4] M. E. Ingebrigtsen, A. Y. Kuznetsov, B. G. Svensson, G. Alfieri, A. Mihaila, U. Badstübner, A. Perron, L. Vines, and J. B. Varley, "Impact of proton irradiation on conductivity and deep level defects in β-Ga_2O_3," APL Mater. **7**, 022510 (2019).

[5] Z. Zhang, E. Farzana, A. R. Arehart, and S. A. Ringel, "Deep level defects throughout the bandgap of (010) β-Ga_2O_3 detected by optically and thermally stimulated defect spectroscopy," Appl. Phys. Lett. **108**, 052105 (2016).

[6] E. Farzana, E. Ahmadi, J. S. Speck, A. R. Arehart, and S. A. Ringel, "Deep level defects in Ge-doped (010) β-Ga_2O_3 layers grown by plasma-assisted molecular beam epitaxy," J. Appl. Phys. **123**, 161410 (2018).

[7] A. Y. Polyakov, N. B. Smirnov, I. V. Shchemerov, D. Gogova, S. A. Tarelkin, and S. J. Pearton, "Compensation and persistent photocapacitance in homoepitaxial Sn-doped β-Ga_2O_3," J. Appl. Phys. **123**, 115702 (2018).

[8] E. Farzana, M. F. Chaiken, T. E. Blue, A. R. Arehart, and S. A. Ringel, "Impact of deep level defects induced by high energy neutron radiation in β-Ga_2O_3," APL Mater. **7**, 022502 (2019).

[9] C. Zimmermann, V. Rønning, Y. Kalmann Frodason, V. Bobal, L. Vines, and J. B. Varley, "Primary intrinsic defects and their charge transition levels in β-Ga_2O_3," Phys. Rev. Mater. **4**, 074605 (2020).

[10] J. B. Varley, H. Peelaers, A. Janotti, and C. G. V. de Walle, "Hydrogenated cation vacancies in semiconducting oxides," J. Phys.: Condens. Matter **23**, 334212 (2011).

[11] F. Tuomisto and I. Makkonen, "Defect identification in semiconductors with positron annihilation: Experiment and theory," Rev. Mod. Phys. **85**, 1583–1631 (2013).

[12] E. Korhonen, F. Tuomisto, D. Gogova, G. Wagner, M. Baldini, Z. Galazka, R. Schewski, and M. Albrecht, "Electrical compensation by Ga vacancies in Ga_2O_3 thin films," Appl. Phys. Lett. **106**, 242103 (2015).

[13] F. Tuomisto, A. Karjalainen, V. Prozheeva, I. Makkonen, G. Wagner, and M. Baldini, "Ga vacancies and electrical compensation in β-Ga_2O_3 thin films studied with positron annihilation spectroscopy," in *Oxide-Based Materials and Devices X* (International Society for Optics and Photonics, 2019), Vol. 10919, p. 1091910.

[14] A. Y. Polyakov, N. B. Smirnov, I. V. Shchemerov, E. B. Yakimov, J. Yang, F. Ren, G. Yang, J. Kim, A. Kuramata, and S. J. Pearton, "Point defect induced degradation of electrical properties of Ga_2O_3 by 10 MeV proton damage," Appl. Phys. Lett. **112**, 032107 (2018).

[15] A. Y. Polyakov, N. B. Smirnov, I. V. Shchemerov, E. B. Yakimov, S. J. Pearton, C. Fares, J. Yang, F. Ren, J. Kim, P. B. Lagov, V. S. Stolbunov, and A. Kochkova, "Defects responsible for charge carrier removal and correlation with deep level introduction in irradiated β-Ga_2O_3," Appl. Phys. Lett. **113**, 092102 (2018).

[16] C. Zimmermann, E. F. Verhoeven, Y. K. Frodason, P. M. Weiser, J. B. Varley, and L. Vines, "Formation and control of the E2* center in implanted β-Ga_2O_3 by reverse-bias and zero-bias annealing," J. Phys. D: Appl. Phys. **53**, 464001 (2020).

[17] J. F. Mcglone, Z. Xia, Y. Zhang, C. Joishi, S. Lodha, S. Rajan, S. A. Ringel, and A. R. Arehart, "Trapping effects in Si δ -doped β-Ga_2O_3 MESFETs on an Fe-doped β-Ga_2O_3 substrate," IEEE Electron Device Lett. **39**, 1042–1045 (2018).

[18] J. F. McGlone, Z. Xia, C. Joishi, S. Lodha, S. Rajan, S. Ringel, and A. R. Arehart, "Identification of critical buffer traps in Si δ-doped β-Ga_2O_3 MESFETs," Appl. Phys. Lett. **115**, 153501 (2019).

[19] Y. K. Frodason, C. Zimmermann, E. F. Verhoeven, P. M. Weiser, L. Vines, and J. B. Varley, "Multistability of isolated and hydrogenated Ga-O divacancies in β-Ga_2O_3," Phys. Rev. Mater. **5**, 025402 (2021).

[20] J. M. Johnson, Z. Chen, J. B. Varley, C. M. Jackson, E. Farzana, Z. Zhang, A. R. Arehart, H.-L. Huang, A. Genc, S. A. Ringel, C. G. Van de Walle, D. A. Muller, and J. Hwang, "Unusual formation of point-defect complexes in the ultrawide-band-gap semiconductor β-Ga_2O_3," Phys. Rev. X **9**, 041027 (2019).

[21] H. J. von Bardeleben, S. Zhou, U. Gerstmann, D. Skachkov, W. R. L. Lambrecht, Q. D. Ho, and P. Deák, "Proton irradiation induced defects in β-Ga_2O_3: A combined EPR and theory study," APL Mater. **7**, 022521 (2019).

Published under an exclusive license by AIP Publishing.

[22]D. Skachkov, W. R. L. Lambrecht, H. J. von Bardeleben, U. Gerstmann, Q. D. Ho, and P. Deák, "Computational identification of Ga-vacancy related electron paramagnetic resonance centers in β-Ga_2O_3," J. Appl. Phys. **125**, 185701 (2019).
[23]N. T. Son, Q. D. Ho, K. Goto, H. Abe, T. Ohshima, B. Monemar, Y. Kumagai, T. Frauenheim, and P. Deák, "Electron paramagnetic resonance and theoretical study of gallium vacancy in β-Ga_2O_3," Appl. Phys. Lett. **117**, 032101 (2020).
[24]A. Karjalainen, V. Prozheeva, K. Simula, I. Makkonen, V. Callewaert, J. B. Varley, and F. Tuomisto, "Split Ga vacancies and the unusually strong anisotropy of positron annihilation spectra in β-Ga_2O_3," Phys. Rev. B **102**, 195207 (2020).
[25]A. Karjalainen, I. Makkonen, J. Etula, K. Goto, H. Murakami, Y. Kumagai, and F. Tuomisto, "Split Ga vacancies in *n*-type and semi-insulating β-Ga_2O_3 single crystals," Appl. Phys. Lett. **118**, 072104 (2021).
[26]P. Weiser, M. Stavola, W. B. Fowler, Y. Qin, and S. Pearton, "Structure and vibrational properties of the dominant OH center in β-Ga_2O_3," Appl. Phys. Lett. **112**, 232104 (2018).
[27]Y. Qin, M. Stavola, W. B. Fowler, P. Weiser, and S. J. Pearton, "Hydrogen centers in β-Ga_2O_3: Infrared spectroscopy and density functional theory," ECS J. Solid State Sci. Technol. **8**, Q3103–Q3110 (2019).
[28]J. R. Ritter, J. Huso, P. T. Dickens, J. B. Varley, K. G. Lynn, and M. D. McCluskey, "Compensation and hydrogen passivation of magnesium acceptors in β-Ga_2O_3," Appl. Phys. Lett. **113**, 052101 (2018).
[29]A. Portoff, A. Venzie, Y. Qin, M. Stavola, W. B. Fowler, and S. J. Pearton, "Vibrational properties of oxygen-hydrogen centers in H^+- and D^+-implanted Ga_2O_3," ECS. J. Solid State Sci. Technol. **9**, 125006 (2020).
[30]S. Ahn, F. Ren, E. Patrick, M. E. Law, S. J. Pearton, and A. Kuramata, "Deuterium incorporation and diffusivity in plasma-exposed bulk Ga_2O_3," Appl. Phys. Lett. **109**, 242108 (2016).
[31]S. Ahn, F. R. E. Patrick, M. E. Law, S. J. Pearton, and A. Kuramata, "Thermal stability of implanted or plasma exposed deuterium in single crystal Ga_2O_3," ECS J. Solid State Sci. Technol. **6**, Q3026–Q3029 (2017).
[32]V. M. Reinertsen, P. M. Weiser, Y. K. Frodason, M. E. Bathen, L. Vines, and K. M. Johansen, "Anisotropic and trap-limited diffusion of hydrogen/deuterium in monoclinic gallium oxide single crystals," Appl. Phys. Lett. **117**, 232106 (2020).
[33]M. Stavola, *Identification of Defects in Semiconductors*, "Semiconductors and Semimetals" (Academic Press, 1999), Vol. 51B.
[34]A. Kyrtsos, M. Matsubara, and E. Bellotti, "Migration mechanisms and diffusion barriers of vacancies in Ga_2O_3," Phys. Rev. B **95**, 245202 (2017).
[35]W. B. Fowler, M. Stavola, Y. Qin, and P. Weiser, "Trapping of multiple H atoms at the Ga(1) vacancy in $\beta-Ga_2O_3$," Appl. Phys. Lett. **117**, 142101 (2020).
[36]I. Makkonen, E. Korhonen, V. Prozheeva, and F. Tuomisto, "Identification of vacancy defect complexes in transparent semiconducting oxides ZnO, In_2O_3 and SnO_2," J. Phys.: Condens. Matter **28**, 224002 (2016).
[37]J. F. Ziegler and J. P. Biersack, "SRIM-2013 software package," see http://www.srim.org (2013).
[38]M. J. Puska, C. Corbel, and R. M. Nieminen, "Positron trapping in semiconductors," Phys. Rev. B **41**, 9980–9993 (1990).
[39]M. D. McCluskey, "Point defects in Ga_2O_3," J. Appl. Phys. **127**, 101101 (2020).
[40]Z. Galazka, K. Irmscher, R. Schewski, I. M. Hanke, M. Pietsch, S. Ganschow, D. Klimm, A. Dittmar, A. Fiedler, T. Schroeder, and M. Bickermann, "Czochralski-grown bulk β-Ga_2O_3 single crystals doped with mono-, di-, tri-, and tetravalent ions," J. Cryst. Growth **529**, 125297 (2020).
[41]A. Kuramata, K. Koshi, S. Watanabe, Y. Yamaoka, T. Masui, and S. Yamakoshi, "High-quality β-Ga_2O_3 single crystals grown by edge-defined film-fed growth," Jpn. J. Appl. Phys. **55**, 1202A2 (2016).
[42]T. Zacherle, P. C. Schmidt, and M. Martin, "*Ab initio* calculations on the defect structure of β-Ga_2O_3," Phys. Rev. B **87**, 235206 (2013).
[43]P. Deák, Q. Duy Ho, F. Seemann, B. Aradi, M. Lorke, and T. Frauenheim, "Choosing the correct hybrid for defect calculations: A case study on intrinsic carrier trapping in β-Ga_2O_3," Phys. Rev. B **95**, 075208 (2017).
[44]J. B. Varley, J. R. Weber, A. Janotti, and C. G. Van de Walle, "Oxygen vacancies and donor impurities in β-Ga_2O_3," Appl. Phys. Lett. **97**, 142106 (2010).

Published under an exclusive license by AIP Publishing.